Neural and Vascular Responses to Fused Binocular Stimuli: A VEP and fNIRS Study

Sobanawartiny Wijeakumar,[1] *Uma Shahani,*[1] *Daphne L. McCulloch,*[1] *and William A. Simpson*[2]

Purpose. The aim of our study was to investigate the correlation between neural and hemodynamic responses to stereoscopic stimuli recorded over visual cortex.

Methods. Test stimuli consisted of a static checkerboard (checks) and dichoptic static random dot (RD) presentations with no binocular disparity (ZD) or with horizontal disparity (HD). Hemodynamic responses were recorded from right and left occipital sites using functional near-infrared spectroscopy (fNIRS). Visual evoked potentials (VEPs) were recorded over three occipital sites to the onset of the same stimuli.

Results. Early components, N1 and P2, were sensitive to HD, suggesting that an enhanced N1-reduced P2 complex could be an indicator of binocular disparity and stereopsis. VEPs to checks and ZD stimulation were similar. fNIRS recordings showed changes in hemodynamic activation from baseline levels in response to all stimuli. In general, HD elicited a larger vascular response than ZD. Oxyhemoglobin concentration (HbO) was correlated with the VEP amplitude during the checks and HD presentations.

Conclusions. We report an association between neural and hemodynamic activation in response to checks and HD. In addition, the results suggested that N1-P2 complex in the VEP could be a neural marker for stereopsis and fNIRS demonstrated differences in HbO. Specifically, checks and HD elicited larger hemodynamic responses than random dot patterns without binocular disparity. (*Invest Ophthalmol Vis Sci.* 2012;53:5881–5889) DOI:10.1167/iovs.12-10399

Depth perception is based on the amalgamation of monocular cues, such as lighting, accommodation, shading, blur, perspective, and motion parallax, and binocular cues, such as convergence and stereopsis. Of these, stereopsis is the principal measure of binocular vision. Multiple studies have used electrophysiologic and psychophysical methods to investigate stereoscopic processing.[1–4] Aspects, such as visual persistence, hemispheric dominancy, position within the visual field, temporal frequency, and depth reversal rates, affected depth perception.[5–9] Visual evoked potential (VEP) studies have implicated the N1 (or an early negative wave) and P3 components to be elicited in the visual cortex by stereo and depth-inducing stimuli.[10–15] In accordance with these results, functional magnetic resonance imaging (fMRI) has shown definitively that areas involved in stereoscopic processing extend from the dorsal occipital[16–18] through to the posterior parietal areas.[16,19–21] The relatively new technique of functional near-infrared spectroscopy (fNIRS) can measure changes in blood flow in response to neural activation as absolute or relative concentrations of oxyhemoglobin (HbO) and deoxyhemoglobin (Hb) levels. fNIRS relies on the principle that amplitude modulated light of two different wavelengths from the near-infrared and visible spectrum will penetrate the scalp and skull through to brain tissue. fNIRS also can be used easily in conjunction with VEPs. In previous studies, we have shown, using fNIRS, early visual processing in response to simple visual stimuli.[22,23] In our study, we used fNIRS and VEPs, respectively, to quantify and correlate the hemodynamic and neural responses to stereopsis. The aims were 3-fold: to identify neural markers within the VEPs in response to stereopsis over the primary visual cortex, to observe absolute changes in hemodynamic activation in response to static stereograms, and to correlate VEPs to hemodynamic activation to understand if the neural and vascular components underlying simple and complex visual stimuli were linearly coupled.

Methods

Observers

Five observers took part in the fNIRS study. Three additional observers were used for the VEP study. All who were recruited either were university students or employees with an age range of 18–32 years. All observers also were tested for suitability by measuring stereo (with the TNO stereo test) and visual acuity (with Bailey Lovie LogMAR charts). The requirements were that the stereo acuity was 60 seconds (") of arc or better and the visual acuity was 6/6 (0.0 LogMAR) or better in each eye. Observers wore appropriate refractive correction if required and had no history of any visual disorders. The experiments were approved by the local Ethics committee and, in accordance with the Declaration of Helsinki, all participants gave their informed consent.

Visual Stimuli

Three types of test stimuli were used consisting of a static checkerboard and two static, red-green random dot (RD) presentations. The checkerboard presentation (checks) matched the ISCEV[24] standard for small check sizes (check width 15 minutes ['] of arc, and >97% contrast). The luminance of the black checks was less than 1 cd/m^2 and the luminance of the white checks was 66 cd/m^2. A luminance-matched grey screen (33 cd/m^2) served as the control presentation for the static checkerboard.

The RD display consisted of 2000 randomly placed red and green squares (3 × 3 mm) subtending 10.3′. Both RD presentations were viewed dichoptically, each through red and green filters. In the zero disparity (ZD) condition the red-green dots when fused appeared as a

From the [1]Glasgow Caledonian University, Vision Sciences, Department of Life Sciences, Glasgow, United Kingdom; and [2]School of Psychology, University of Plymouth, Drake Circus, Plymouth, United Kingdom.

Supported by Fight for Sight (SW).

Submitted for publication June 14, 2012; revised July 24, 2012; accepted July 27, 2012.

Disclosure: **S. Wijeakumar**, None; **U. Shahani**, None; **D.L. McCulloch**, None; **W.A. Simpson**, None

Corresponding author: Sobanawartiny Wijeakumar, Department of Vision Sciences, Glasgow Caledonian University, 70 Cowcaddens Road, G4 0BA, Glasgow, Scotland, UK; swijea11@gcal.ac.uk.

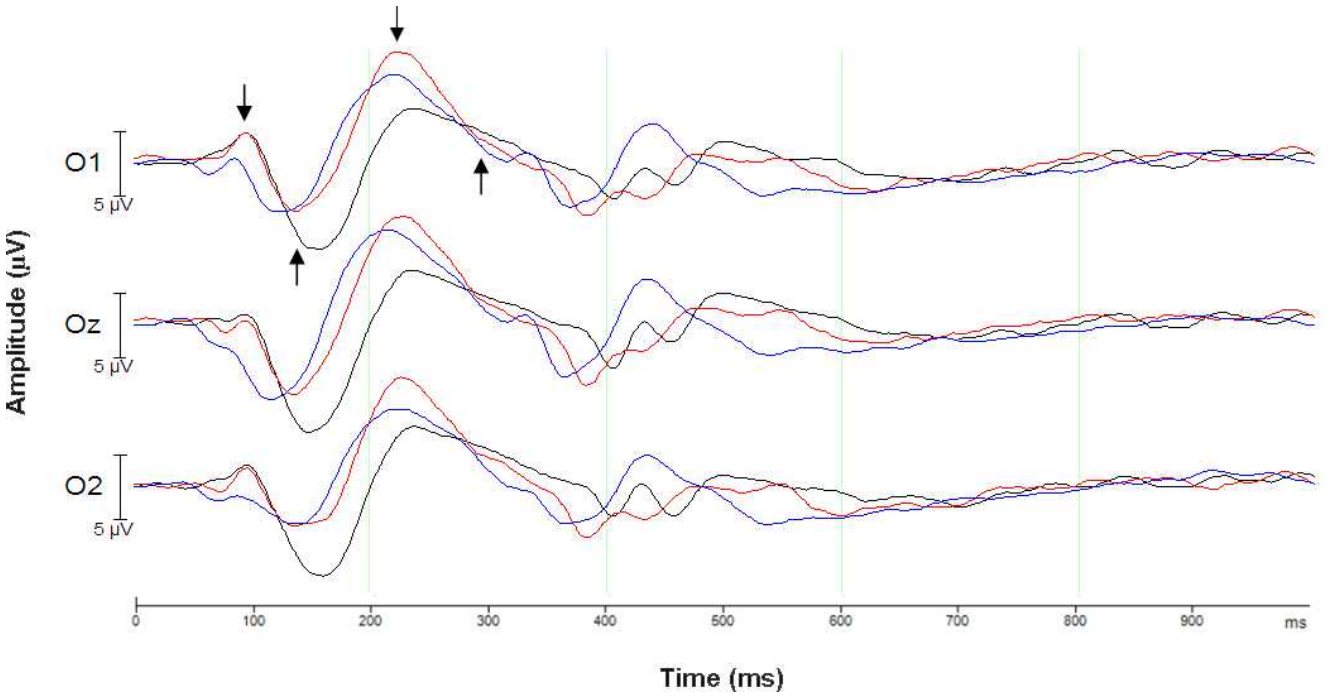

Figure 1. Group averaged VEPs in response to checks (*blue*), ZD (*red*) and HD (*black*) at locations O_1, O_z, and O_2 ($n = 9$). *Arrows*: mean locations for P1, N1, P2, and N2 across all three stimuli.

"flat" surface and, in the horizontal disparity (HD) condition, the red-green dots when fused produced horizontal disparity in bands across the screen, which appeared as horizontal sinusoidal corrugations. From the peak to the trough of the sinusoidal pattern, the maximum disparity was 11′. At the test distance of 1 meter, the visual field was 20.7° × 15.4°. Both RD presentations used black screens as control stimuli. The observers were asked to fixate on a small cross, presented at the center of the screen.

VEP Recordings

VEPs were recorded using the Brain Vision recorder (Brain Products Ltd., Munich, Germany) with arrangement of Ag/AgCl electrode (actiCAP System; Brain Products Ltd.) based on the International 10–20 System of Electrode Placement. Recordings from occipital locations O_1, O_z, and O_2 were compared to fNIRS recordings. Data were sampled at 1 KHz, and band-pass filtered between 0.15 and 100 Hz. Horizontal and vertical electro-oculograms (EOGs) also were obtained to correct for blink artifacts. All electrode impedances were maintained below 10 KΩ. VEPs were averaged in response to 100 stimulus presentations. Each duty cycle lasted for 1000 ms (test stimulus presentation of 250 ms followed by a blank screen presentation for 750 ms).

fNIRS Recordings

A two-channel fNIRS oximeter (OxiplexTS ISS, Inc., Champaign, IL) was used to measure absolute changes in hemoglobin concentrations. Eight sources were modulated at 110 MHz, and emitted light at 834 and 692 nm (four sources for each wavelength). The sensor was a flat flexible pad that housed a detector and four emitter pairs at fixed distances from each other (1.93–3.51 cm). The attenuated light after passing through layers of scalp and cortex was detected. The fixed distances between each of the emitter-detector pairs were used to calculate the slopes of averaged light intensity (DC), modulated intensity (AC), and the phase. These values were converted to absolute concentrations of HbO and Hb using a modified version of the Beer-Lambert Law. Total hemoglobin concentration (THb) was calculated to be the summation of HbO and Hb. We report from only the left and right occipital locations O_1 and O_2 as those locations overlying the midline produced nonsignificant fNIRS responses.[22] Each observer was presented with a 10-minute trial for each of the three stimuli. Each trial consisted of 10 one-minute long segments (30 seconds of test stimulus presentation followed by 30 seconds of control stimulus presentation). Observers were instructed to perform a simple button-press task whenever the presentation changed to sustain their attention.

Data Analysis

For the VEP analysis, the data were analyzed using the BrainVision analyzer (Brain Products Ltd., London, UK). Each trial (1000 ms) was averaged within each observer and a grand average was calculated. Implicit times and amplitudes were calculated for four components, namely P1 (50–150 ms), N1 (120–200 ms), P2 (170–250 ms), and N2 (270–330 ms). For the fNIRS analysis, one-minute segments were averaged within each observer and across observers. The amplitude values recorded during the last 16 seconds of the test and control stimulus presentations for each one-minute segment were used. Comparisons for each chromophore were made between conditions (control and test presentations), stimuli, and locations across observers. SPSS 16 was used to perform repeated measures ANOVAs on the VEPs and fNIRS data separately. Greenhouse-Geisser correction epsilon was used in cases where the Mauchly's sphericity test for normality was violated to correct the degrees of freedom. Subsequent post-hoc analysis with pairwise comparisons was done wherever necessary using Bonferroni corrections. In general, HbO responses were the most stable of the three chromophores. Therefore, a one-tailed bivariate Pearson's correlation of coefficient was used to correlate the HbO and VEP responses.

Results

VEP Recordings

Four components were identifiable within the majority of VEP waveforms. Figure 1 shows the averaged VEPs in response to

checks (blue line), ZD (red line), and HD (black line) at locations O_1, O_z, and O_2. Table 1 shows summarized mean (± SEM) values for N1 and P2 implicit times and amplitudes. P1 and N2 components were variable and did not show significant differences between stimuli.

The main effects of stimulus for N1 implicit times ($F[2, 12] = 11$, $P < 0.05$), P2 implicit times ($F[2, 9] = 13$, $P < 0.01$), and P2 amplitude ($F[2, 9]P < 0.05$) were significant. Specifically, P2 was seen to be relatively delayed in HD and ZD conditions than for checks ($P < 0.05$). Furthermore, ZD elicited a larger P2 than HD at all three occipital locations ($P < 0.05$).

Subsequent post-hoc pairwise comparisons revealed that the N1 occurred much later in response to HD than for checks at O_z and O_2 ($P < 0.05$). This component also occurred later for ZD relative to the response to checks at O_1 ($P > 0.05$). Additionally, when the data from locations were pooled together, the N1 was later for HD than for checks ($P < 0.05$). A larger N1 component also was observed for HD than for ZD at O_z ($P < 0.05$). Pairwise comparisons revealed that the P2 occurred later in response to HD than for checks at location O_z ($P < 0.05$).

Table 1. Implicit Times and Amplitudes of VEP Components N1 and P2

	Implicit Times (ms) Mean ± SEM						Amplitude (μV) Mean ± SEM					
	N1			P2			N1			P2		
	O_1	O_z	O_2	O_1	O_z	O_2	O_1	O_z	O_2	O_1	O_z	O_2
HD	179 ± 23	155 ± 6	162 ± 5	261 ± 13	259 ± 12	259 ± 11	−7.5 ± 1.4	−8.9 ± 1.5	−8.0 ± 2.0	5.97 ± 1.56	6.0 ± 1.5	6.9 ± 1.4
ZD	143 ± 5	141 ± 4	139 ± 9	235 ± 6	237 ± 7	234 ± 6	−5.6 ± 1.2	−6.4 ± 1.4	−5.9 ± 1.5	9.67 ± 1.80	9.6 ± 1.7	9.7 ± 1.5
Checks	128 ± 6	114 ± 6	125 ± 7	215 ± 9	198 ± 17	224 ± 11	−5.5 ± 1.8	−7.9 ± 2.1	−4.7 ± 2.1	8.62 ± 0.8	8.6 ± 1.3	8.5 ± 1.2

fNIRS Recordings

Increases in HbO and THb concentrations were observed in response to all three stimuli at both locations. As expected, Hb concentration dropped during stimulation. It took 10 to 12 seconds for the HbO response to rise and reach a plateau. This was maintained until approximately 5 seconds following offset when values returned to baseline levels. Figure 2 shows the HbO, Hb, and THb responses after averaging within each observer and across observers in response to checks, ZD, and HD. Table 2 shows mean ± SEM values for change in HbO, Hb, and THb concentrations.

A three-factor ANOVA model with factors of condition (ON/OFF), stimulus (checks/ZD/HD), and location (O_1/O_2) was used. A summary of the results for the main effects and post-hoc analyses are presented in Table 3. All three chromophores showed larger concentrations at O_1 than at O_2 ($P < 0.05$). Also, responses to HD were larger than those to ZD ($P < 0.05$). Post-hoc pairwise comparisons between conditions revealed significantly higher amplitudes during the test stimulus presentation than the control stimulus presentation across locations, stimuli, and chromophores ($P < 0.05$). Pairwise comparisons between locations showed that the response at O_1 was higher than that at O_2 only for the checks stimulus for HbO and THb concentrations ($P < 0.05$). On the other hand, the change in Hb concentration at O_1 was larger than that at O_2 for ZD and HD presentations ($P < 0.05$). Pairwise comparisons between stimuli revealed that for HbO and THb concentrations, larger amplitude levels were observed for checks than for HD at O_1 ($P < 0.05$). Additionally for THb, the response to HD was larger than ZD at O_1 and larger than for checks at O_2 ($P < 0.05$).

Correlation between VEPs and HbO Response

Large VEPs were associated with large vascular responses. Root mean square (RMS) values of the HbO response (HbO_{RMS}) were calculated for a time window of the last 16 seconds of the test stimulus presentation for each of the one-minute segments for each observer at each location. For the VEPs (VEP_{RMS}), each trial was split into 10 sections where each section was an average of 10 segments. RMS values were calculated for a time window between 50 and 330 ms after pattern onset for each section and for each observer at each location (10 RMS values × 5 observers for O_1, O_2, and O_z). The correlation between VEP_{RMS} and HbO_{RMS} for checks and HD was significant at O_1

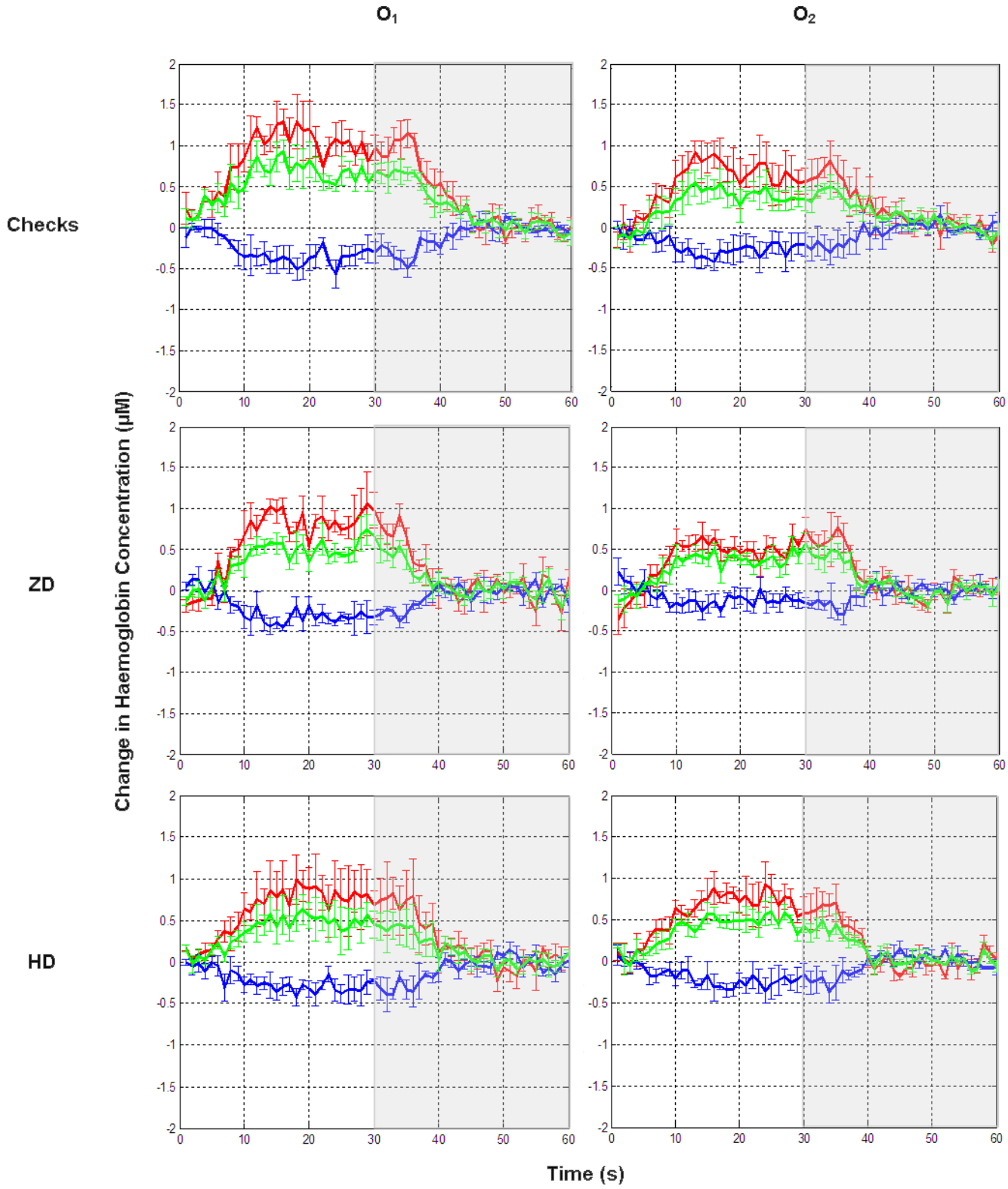

Figure 2. Averaged change in HbO (*red line*), Hb (*blue line*), and THb (*green line*) concentrations (*left column*, O_1; *right column*, O_2) from black/grey screen presentation. *White area* shows the period of test stimulus presentation. *Grey shaded area* shows the period of control stimulus presentation (*grey/black screen*). *Top, middle*, and *bottom rows* show the changes in hemoglobin concentration in response to checks, ZD, and HD, respectively ($n = 5$).

Table 2. Changes in HbO, Hb, and THb Concentrations at Occipital Locations (Mean ± SEM)

			Checks	ZD	HD
Change in chromophore concentration from control stimulation (μM)	HbO	O_1	0.92 ± 0.06	0.64 ± 0.03	0.77 ± 0.05
		O_2	0.62 ± 0.05	0.61 ± 0.03	0.73 ± 0.03
	Hb	O_1	−0.30 ± 0.03	−0.26 ± 0.01	−0.35 ± 0.02
		O_2	−0.23 ± 0.03	−0.18 ± 0.02	−0.26 ± 0.02
	THb	O_1	0.58 ± 0.04	0.37 ± 0.02	0.51 ± 0.04
		O_2	0.35 ± 0.03	0.39 ± 0.04	0.45 ± 0.02

and O_2 (checks at O_1 $r^2 = 0.45$, $P < 0.005$; checks at O_2 $r^2 = 0.30$, $P < 0.05$; HD at O_1 $r^2 = 0.46$, $P < 0.001$; HD at O_2 $r^2 = 0.36$. $P < 0.01$, Figs. 3a–3d). Furthermore, VEP_{RMS} at O_z was significantly correlated with HbO_{RMS} averaged across O_1 and O_2 ($O_1 + O_2/2$) for checks ($r^2 = 0.57$, $P < 0.001$) and HD ($r^2 = 0.60$, $P < 0.001$, Figs. 3e, 3f). None of the correlations achieved significance for ZD.

Discussion

VEPs and fNIRS measure different aspects of brain function. Neural activation of the cortex, which occurs within 50 to 100 ms after stimulus onset, is represented by the former. On the other hand, fNIRS measures the slow vascular changes as a consequence of neural activation with a latency of several seconds.

Evoked Potentials to Static Pattern Onset Stimulation

Typically, VEPs have complex waveforms with several components. Early components (>200 ms) are said to be involved in the primary stages of visual processing of any stimulus, and are known to originate from magnocellular and parvocellular pathways.[25–28] Some studies also have shown associations between the early P1 and non-stereoscopic depth.[29–31] Omoto et al. used figures where smaller squares made up bigger squares to create 2D and 3D images with a concave or a convex effect, and observed an enhanced P1 peak over the temporal-parietal-occipital regions for the latter.[30] However, in our current study, no significant differences in P1 were observed across stimuli suggesting that the underlying early pattern processing mechanisms were similar for each of the three stimuli.

An early negative VEP component has been implicated in studies examining the neural correlates of depth perception using monocular cues, like perspective,[14] and binocular cues, such as chromostereopsis.[15] These studies report source generators of depth processing to be located along the occipital and parietal junctions. Sahinoglu et al. in 2002 used dynamic RD stereogram presentations with convergent disparities to identify an N1 peak (200–400 ms) whose peak latency and amplitude changed with increasing disparity.[32] Many other studies also have reported a similar effect on the early negativity.[33–39] In our current study, an enhanced N1 peak was observed in response to the HD condition, which appeared as a surface corrugated in depth, compared to the ZD condition, which was a fusible flat surface. An enhancement of the N1 component also has been implicated strongly in studies investigating attentional mechanisms.[40,41] However, Cauquil et al. in 2006 reported no effect of attention on the N1 component in a paradigm where 2D and 3D perspective cues (monocular) were presented.[14] In agreement with the results from our study, an enhanced N1 was observed in response to 3D rather than for 2D stimulation. Thus, we support the suggestions made in previous studies of depth perception that N1 might be a marker for neural circuitry involved in depth processing. In our study, the P2 peak amplitude was reduced in response to HD. In contrast, Omoto et al., who used non-stereoscopic stimuli with concave and convex surfaces to induce the perception of depth, reported enhanced P1 and P2 amplitudes.[30] Our results also may be interpreted as showing

Table 3. Summary of Statistical Analyses on fNIRS Measures

	Hemodynamic Response		
	HbO	**THb**	**Hb**
Stimulus	HD > ZD*	HD > ZD*	HD > ZD*
Location	$O_1 > O_2$*	$O_1 > O_2$*	$O_1 > O_2$*
Condition	Test > Control*	Test > Control*	Test > Control*
Stimulus × Location	*	*	NS
Stimulus × Condition	NS	NS	*
Location × Condition	*	*	*
Stimulus × Location × Condition	For checks : $O_1 > O_2$* For O_1 : checks > HD*	For checks : $O_1 > O_2$* For O_1 : checks > HD* For O_1 : HD > ZD* For O_2 : HD > checks*	For HD and ZD : $O_1 > O_2$*

HbO and THb: Significant main effects of stimulus – for HbO, $F(2, 154) = 7$, $P < 0.05$ and for THb, $F(2, 135) = 6$, $P < 0.05$; location – for HbO, $F(1, 79) = 7$, $P < 0.05$ and for THb, $F(2, 135) = 10$, $P < 0.05$; condition – for HbO, $F(1, 79) = 584$, $P < 0.05$ and for THb, $F(1,79) = 408$, $P < 0.05$; interactions between stimulus and location – for HbO, $F(2, 150) = 5$, $P < 0.05$ and for THb, $F(2, 155) = 3$, $P < 0.05$; location and condition – for HbO, $F(1, 79) = 11$, $P < 0.05$ and for THb, $F(1, 79) = 5$, $P < 0.05$; and stimulus location and condition – for HbO, $F(2, 151) = 7$, $P < 0.05$, and for THb, $F(2, 144) = 5$, $P < 0.05$.

Hb: Significant main effects of stimulus – $F(2, 152) = 3$, $P < 0.05$; condition – $F(1, 79) = 283$, $P < 0.05$; and location $F(1, 79) = 11$, $P < 0.05$; and significant interactions between stimulus and condition – $F(2, 135) = 5$, $P < 0.05$, and location and condition $F(1, 79) = 17$, $P < 0.05$.

* A significance of less than 0.05.

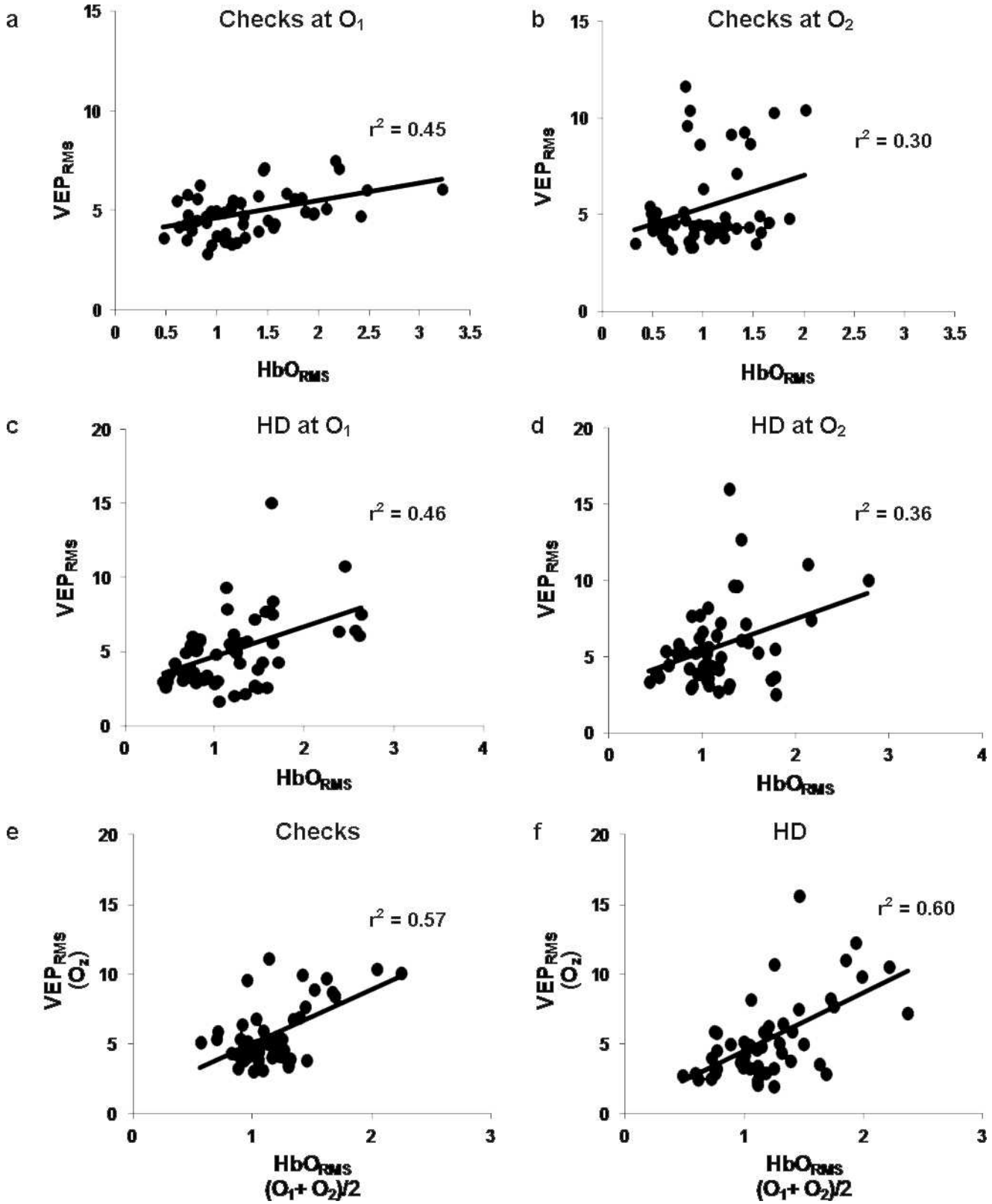

Figure 3. VEP_{RMS} was correlated with HbO_{RMS} for checks (**a**, **b**) and HD (**c**, **d**) at O_1 and O_2. The VEP_{RMS} at O_z was correlated with HbO_{RMS} averaged across O_1 and O_2 ($[O_1+O_2]/2$) for (**e**) checks and (**f**) HD.

that N1-P2 complex could collectively represent stereoscopic depth processing.

Hemodynamic Activation in Response to Static Pattern Stimulation

Visual stimuli including checkerboards,[22,23,42–47] rotating shapes,[48,49] peripheral drift illusion,[50] and faces,[51–55] elicit hemodynamic activation. As expected, a change in hemodynamic activation was observed in response to all stimuli relative to the baseline levels to blank screen presentations. The response characteristics of the averaged waveform (time taken to plateau and recovery to baseline levels) displayed similar trends to those previously reported in response to simple checkerboard stimulation. This held true for all chromophores measured.

fMRI studies of stereoscopic processing have shown involvement of the dorsal region of the occipital cortex[16,56,57] and other parts of the visual cortex.[18,21,58,59] Comparing activated areas in response to static and dynamic stereopsis, Iwami et al. found that the dorsal parieto-occipital region was a common processing area. Area V3A is reported to produce the largest response when random dot presentation with disparity was alternated with zero disparity.[18,60] Tsao et al. in 2003 compared activated areas in humans and macaques in response to disparity-defined checkerboards formed with random dot presentations.[21] They found activation in V3, V4d, and V7 of the visual cortex. We suggested that along with pattern-sensitive and binocularly-active neurons, disparity-sensitive cells must have accounted for the increased activation leading to the hemodynamic responses recorded over the occipital scalp across both hemispheres. This could be explained by increased hemodynamic activation from the disparity sensitive neurons of the visual cortex adding to the responses of neurons tuned to other stimulus features, such as contrast and color.

Correlation between VEPs and HbO Concentration

Previously, studies combining fNIRS and electrophysiology have used different kinds of stimulation to investigate elements of neurovascular coupling.[61–65] Some others also have tried to correlate the "fast" signal or the Event-related optical signal[66] to VEPs. A study by Obrig et al. showed coupling between fNIRS and VEP measures in response to a reversing checkerboard stimulus.[62] They correlated absolute measures of chromophore concentrations with peak-to-peak amplitude values. Similar results were observed by Syre et al. when they correlated VEPs with fNIRS in response to a reversing checkerboard across three different stimulus train durations.[67] These results were in accordance with those of Rovati et al., who correlated VEPs and fNIRS responses across different contrast levels. We explored neuro-vascular elements underlying stereopsis. The linear correlation between fNIRS and VEP measures was significant for stimuli with a range of attributes, such as contrast, sharp edges (corrugations), and disparity accounting for up to 30% to 46% of the variance in the data. These stimuli could activate pools of neurons and subsequently induce a vascular response. The flat stimulus ZD lacked disparity and internal structure (sharp corrugations) elicited increased hemodynamic responses, but these were not correlated with VEP amplitude. Finally, the VEP amplitude at O_z was correlated with the HbO responses from O_1 and O_2 for the same stimuli. The VEP at the midline[68] is well-modeled as the vector sum of the responses from the right and left occipital cortices. A strong correlation between O_z, and the average of O_1 and O_2 is a good indication of the overall associations between neural and vascular activation.[69,70]

In summary, specific changes were observed across both VEPs and hemoglobin concentration levels in response to onset and static stimulation. In agreement with previous studies, we suggested that the N1-P2 complex could be a marker of stereopsis in V1. A larger change in hemodynamic activation was observed for RD presentations with a 3D corrugated surface compared to presentations of a flat surface. Finally, VEP amplitudes were correlated with HbO concentration for complex stimuli across two occipital locations. It would be interesting to investigate the effects of stereopsis on neural and hemodynamic activation across occipital-parietal-temporal junctions.

References

1. Livingstone MS, Hubel DH. Stereopsis and positional acuity under dark adaptation. *Vision Res*. 1994;34:799–802.
2. Manning ML, Finlay DC, Dewis SA, Dunlop DB. Detection duration thresholds and evoked potential measures of stereosensitivity. *Doc Ophthalmol*. 1992;79:161–175.
3. Livingstone MS, Hubel DH. Psychophysical evidence for separate channels for the perception of form, color, movement, and depth. *J Neurosci*. 1987;7:3416–3468.
4. Hubel D. *Eye, Brain And Vision*. San Francisco: W. H. Freeman; 1988.
5. Skrandies W. Assessment of depth perception using psychophysical thresholds and stereoscopically evoked brain activity. *Doc Ophthalmol*. 2009;119:209–216.
6. Skrandies W. The processing of stereoscopic information in human visual cortex: psychophysical and electrophysiological evidence. *Clin Electroencephalogr*. 2001;32:152–159.
7. Skrandies W. Depth perception and evoked brain activity: the influence of horizontal disparity and visual field location. *Vis Neurosci*. 1997;14:527–532.
8. Skrandies W. Contrast and stereoscopic visual stimuli yield lateralized scalp potential fields associated with different neural generators. *Electroencephalogr Clin Neurophysiol*. 1991;78:274–283.
9. Skrandies W. Visual persistence of stereoscopic stimuli: electric brain activity without perceptual correlate. *Vision Res*. 1987;27:2109–2118.
10. Mol J, Caberg HB. Contingent stereoptic variation as a response to moving random-dot stereograms. *Electroencephalogr Clin Neurophysiol*. 1977;43:513.
11. Iizuka K. Depth perception and amplitude of VEPs for variations of dot density in static random dot stereograms. *Nihon Ganka Gakkai Zasshi*. 1992;96:985–992.
12. Fukai S. Topographic visually evoked potentials induced by stereoptic stimulus. *Br J Ophthalmol*. 1985;69:612–617.
13. Hu C, Yang DS, Li X. Stereoscopic visual evoked potential elicited by static random dot stereogram. *Zhonghua Yan Ke Za Zhi*. 1994;30:286–288.
14. Séverac Cauquil A, Trotter Y, Taylor MJ. At what stage of neural processing do perspective depth cues make a difference? *Exp Brain Res*. 2006;170:457–463.
15. Cauquil AS, Delaux S, Lestringant R, Taylor MJ, Trotter Y. Neural correlates of chromostereopsis: an evoked potential study. *Neuropsychologia*. 2009;47:2677–2681.
16. Nishida Y, Hayashi O, Iwami T, et al. Stereopsis-processing regions in the human parieto-occipital cortex. *Neuroreport*. 2001;12:2259–2263.
17. Nishida S, Sasaki Y, Murakami I, Watanabe T, Tootell RB. Neuroimaging of direction-selective mechanisms for second-order motion. *J Neurophysiol*. 2003;90:3242–3254.
18. Backus BT, Fleet DJ, Parker AJ, Heeger DJ. Human cortical activity correlates with stereoscopic depth perception. *J Neurophysiol*. 2001;86:2054–2068.

19. Durand JB, Peeters R, Norman JF, Todd JT, Orban GA. Parietal regions processing visual 3D shape extracted from disparity. *Neuroimage*. 2009;46:1114–1126.
20. Durand JB, Nelissen K, Joly O, et al. Anterior regions of monkey parietal cortex process visual 3D shape. *Neuron*. 2007;55:493–505.
21. Tsao DY, Vanduffel W, Sasaki Y, et al. Stereopsis activates V3A and caudal intraparietal areas in macaques and humans. *Neuron*. 2003;39:555–568.
22. Wijeakumar S, Shahani U, Simpson WA, McCulloch DL. Localization of hemodynamic responses to simple visual stimulation: an fNIRS study. *Invest Ophthalmol Vis Sci*. 2012;53:2266–2273.
23. McIntosh MA, Shahani U, Boulton RG, McCulloch DL. Absolute quantification of oxygenated hemoglobin within the visual cortex with functional near infrared spectroscopy (fNIRS). *Invest Ophthalmol Vis Sci*. 2010;51:4856–4860.
24. Odom JV, Bach M, Brigell M, et al. ISCEV standard for clinical visual evoked potentials (2009 update). *Doc Ophthalmol*. 2009;120:111–119.
25. Woldorff MG, Fox PT, Matzke M, et al. Retinotopic organization of early visual spatial attention effects as revealed by PET and ERPs. *Hum Brain Mapp*. 1997;5:280–286.
26. Simpson GV, Pflieger ME, Foxe JJ, et al. Dynamic neuroimaging of brain function. *J Clin Neurophysiol*. 1995;12:432–449.
27. Ducati A, Fava E, Motti ED. Neuronal generators of the visual evoked potentials: intracerebral recording in awake humans. *Electroencephalogr Clin Neurophysiol*. 1988;71:89–99.
28. Murray MM, Foxe JJ, Higgins BA, Javitt DC, Schroeder CE. Visuo-spatial neural response interactions in early cortical processing during a simple reaction time task: a high-density electrical mapping study. *Neuropsychologia*. 2001;39:828–844.
29. Parks NA, Corballis PM. Attending to depth: electrophysiological evidence for a viewer-centered asymmetry. *Neuroreport*. 2006;17:643–647.
30. Omoto S, Kuroiwa Y, Otsuka S, et al. P1 and P2 components of human visual evoked potentials are modulated by depth perception of 3-dimensional images. *Clin Neurophysiol*. 2010; 121:386–391.
31. Hayashi E, Kuroiwa Y, Omoto S, Kamitani T, Li M, Koyano S. Visual evoked potential changes related to illusory perception in normal human subjects. *Neurosci Lett*. 2004;359:29–32.
32. Sahinoglu B. The effect of disparity change on binocular visual evoked potential parameters elicited by convergent dynamic random-dot stereogram stimuli in humans. *Eur J Appl Physiol*. 2002;88:178–184.
33. Regan D, Beverley KI. Electrophysiological evidence for existence of neurones sensitive to direction of depth movement. *Nature*. 1973;246:504–506.
34. Fenelon B, Neill RA, White CT. Evoked potentials to dynamic random dot stereograms in upper, center and lower fields. *Doc Ophthalmol*. 1986;63:151–156.
35. Chao GM, Odom JV, Karr D. Dynamic stereoacuity: a comparison of electrophysiological and psychophysical responses in normal and stereoblind observers. *Doc Ophthalmol*. 1988;70:45–58.
36. Wang G, Kameda S. Event-related potential component associated with the recognition of three-dimensional objects. *Neuroreport*. 2005;16:767–771.
37. Neill RA, Fenelon B. Scalp response topography to dynamic random dot stereograms. *Electroencephalogr Clin Neurophysiol*. 1988;69:209–217.
38. Janssen P, Vogels R, Orban GA. Macaque inferior temporal neurons are selective for disparity-defined three-dimensional shapes. *Proc Natl Acad Sci U S A*. 1999;96:8217–8222.
39. Hou C, Pettet MW, Vildavski VY, Norcia AM. Neural correlates of shape-from-shading. *Vision Res*. 2006;46:1080–1090.
40. Martinez A, Teder-Sälejärvi W, Vazquez M, et al. Objects are highlighted by spatial attention. *J Cogn Neurosci*. 2006;18: 298–310.
41. Anllo-Vento L, Hillyard SA. Selective attention to the color and direction of moving stimuli: electrophysiological correlates of hierarchical feature selection. *Percept Psychophys*. 1996;58: 191–206.
42. Watanabe H, Homae F, Nakano T, Taga G. Functional activation in diverse regions of the developing brain of human infants. *Neuroimage*. 2008;43:346–357.
43. Toronov VY, Zhang X, Webb AG. A spatial and temporal comparison of hemodynamic signals measured using optical and functional magnetic resonance imaging during activation in the human primary visual cortex. *Neuroimage*. 2007;34: 1136–1148.
44. Takahashi K, Ogata S, Atsumi Y, et al. Activation of the visual cortex imaged by 24-channel near-infrared spectroscopy. *J Biomed Opt*. 2000;5:93–96.
45. Plichta MM, Heinzel S, Ehlis AC, Pauli P, Fallgatter AJ. Model-based analysis of rapid event-related functional near-infrared spectroscopy (NIRS) data: a parametric validation study. *Neuroimage*. 2007;35:625–634.
46. Tang L, Avison MJ, Gore JC. Nonlinear blood oxygen level-dependent responses for transient activations and deactivations in V1 – insights into the hemodynamic response function with the balloon model. *Magn Reson Imaging*. 2009;27:449–459.
47. Radhakrishnan H, Vanduffel W, Deng HP, Ekstrom L, Boas DA, Franceschini MA. Fast optical signal not detected in awake behaving monkeys. *Neuroimage*. 2009;45:410–419.
48. Széles JC, Litscher G. Objectivation of cerebral effects with a new continuous electrical auricular stimulation technique for pain management. *Neurol Res*. 2004;26:797–800.
49. Schroeter ML, Bücheler MM, Müller K, et al. Towards a standard analysis for functional near-infrared imaging. *Neuroimage*. 2004;21:283–290.
50. Hashimoto T, Minagawa-Kawai Y, Kojima S. Motion illusion activates the visual motion area of the brain: a near-infrared spectroscopy (NIRS) study. *Brain Res*. 2006;1077:116–122.
51. Otsuka Y, Nakato E, Kanazawa S, Yamaguchi MK, Watanabe S, Kakigi R. Neural activation to upright and inverted faces in infants measured by near infrared spectroscopy. *Neuroimage*. 2007;34:399–406.
52. Mitsuda T, Yoshida R. Application of near-infrared spectroscopy to measuring of attractiveness of opposite-sex faces. *Conf Proc IEEE Eng Med Biol Soc*. 2005;6:5900–5903.
53. Marumo K, Takizawa R, Kawakubo Y, Onitsuka T, Kasai K. Gender difference in right lateral prefrontal hemodynamic response while viewing fearful faces: a multi-channel near-infrared spectroscopy study. *Neurosci Res*. 2009;63:89–94.
54. Carlsson J, Lagercrantz H, Olson L, Printz G, Bartocci M. Activation of the right fronto-temporal cortex during maternal facial recognition in young infants. *Acta Paediatr*. 2008;97: 1221–1225.
55. Kobayashi M, Otsuka Y, Nakato E, Kanazawa S, Yamaguchi MK, Kakigi R. Do infants recognize the Arcimboldo images as faces? Behavioral and near-infrared spectroscopic study. *J Exp Child Psychol*. 2011;111:22–36.
56. Smith AT, Wall MB. Sensitivity of human visual cortical areas to the stereoscopic depth of a moving stimulus. *J Vis*. 2008;8:1–12.
57. Bridge H, Parker AJ. Topographical representation of binocular depth in the human visual cortex using fMRI. *J Vis*. 2007;7: 15.1–15.14.

58. Negawa T, Mizuno S, Hahashi T, et al. M pathway and areas 44 and 45 are involved in stereoscopic recognition based on binocular disparity. *Jpn J Physiol*. 2002;52:191–198.
59. Iwami T, Nishida Y, Hayashi O, et al. Common neural processing regions for dynamic and static stereopsis in human parieto-occipital cortices. *Neurosci Lett*. 2002;327:29–32.
60. Rutschmann RM, Greenlee MW. BOLD response in dorsal areas varies with relative disparity level. *Neuroreport*. 2004;15:615–619.
61. Rovati L, Salvatori G, Bulf L, Fonda S. Optical and electrical recording of neural activity evoked by graded contrast visual stimulus. *Biomed Eng Online*. 2007;6:28.
62. Obrig H, Israel H, Kohl-Bareis M, et al. Habituation of the visually evoked potential and its vascular response: implications for neurovascular coupling in the healthy adult. *Neuroimage*. 2002;17:1–18.
63. Horovitz SG, Gore JC. Simultaneous event-related potential and near-infrared spectroscopic studies of semantic processing. *Hum Brain Mapp*. 2004;22:110–115.
64. Zhai J, Li T, Zhang Z, Gong H. Hemodynamic and electrophysiological signals of conflict processing in the Chinese-character Stroop task: a simultaneous near-infrared spectroscopy and event-related potential study. *J Biomed Opt*. 2009;14:054022.
65. Nasi T, Kotilahti K, Noponen T, Nissilä I, Lipiainen L, Merilainen P. Correlation of visual-evoked hemodynamic responses and potentials in human brain. *Exp Brain Res*. 2010;202:561–570.
66. Hueber DM, Franceschini MA, Ma HY, et al. Non-invasive and quantitative near-infrared haemoglobin spectrometry in the piglet brain during hypoxic stress, using a frequency-domain multidistance instrument. *Phys Med Biol*. 2001;46:41–62.
67. Syré F, Obrig H, Steinbrink J, Kohl M, Wenzel R, Villringer A. Are VEP correlated fast optical signals detectable in the human adult by non-invasive nearinfrared spectroscopy (NIRS)? *Adv Exp Med Biol*. 2003;530:421–431.
68. Inoue Y, Sakihara K, Gunji A, et al. Reduced prefrontal hemodynamic response in children with ADHD during the Go/NoGo task: a NIRS study. *Neuroreport*. 2012;23:55–60.
69. Edwards L, Drasdo N. Scalp distribution of visual evoked potentials to foveal pattern and luminance stimuli. *Doc Ophthalmol*. 1987;66:301–311.
70. Bradnam MS, Montgomery DM, Evans AL, et al. Objective detection of hemifield and quadrantic field defects by visual evoked cortical potentials. *Br J Ophthalmol*. 1996;80:297–303.